

Spatial correlations in glass-forming liquids across the mode-coupling crossover

Walter Kob

Laboratoire Charles Coulomb, UMR CNRS 5221, Université Montpellier 2, 34095 Montpellier, France

Sándalo Roldán-Vargas

Laboratoire Charles Coulomb, UMR CNRS 5221, Université Montpellier 2, 34095 Montpellier, France

Departamento de Física Aplicada, Grupo de Física de Fluidos y Biocoloides, Universidad de Granada, 18071 Granada, Spain

Ludovic Berthier

Laboratoire Charles Coulomb, UMR CNRS 5221, Université Montpellier 2, 34095 Montpellier, France

Abstract

We discuss a novel approach, the point-to-set correlation functions, that allows to determine relevant static and dynamic length scales in glass-forming liquids. We find that static length scales increase monotonically when the temperature is lowered, whereas the measured dynamic length scale shows a maximum around the critical temperature of mode-coupling theory. We show that a similar non-monotonicity is found in the temperature evolution of certain finite size effects in the relaxation dynamics. These two independent sets of results demonstrate the existence of a change in the transport mechanism when the glass-former is cooled from moderately to deeply supercooled states across the mode-coupling crossover and clarify the status of the theoretical calculations done at the mean field level.

Keywords: glass transition, computer simulations, liquids, structure, dynamics

PACS: 61.20.Ja, 61.43.Fs

1. Introduction

Within the last 15 years intensive investigations have shown that glass-forming systems have a heterogeneous relaxation dynamics, i.e. that at any given time there are regions in space in which the dynamics is significantly faster than the average dynamics and other regions in which it is slower [1, 2, 3]. Although at the beginning these dynamical heterogeneities were considered to be just an oddity of glass-formers, it has subsequently been understood that they are likely to hold an important key to our understanding for the slowing down of the relaxation dynamics in such systems. This insight has led to a very strong research activity in which the properties of dynamic heterogeneities have been investigated in great detail [4]. These studies have given evidence that the number of particles participating in the collective motion associated with dynamic heterogeneity increases with decreasing temperature from $O(1)$ to $O(10^3)$ if T is lowered from normal liquid temperatures down to T_g [5, 6]. As a consequence these domains can be characterized by a *dynamical* length scale that grows if T is lowered [4, 7].

This growth is in qualitative agreement with mean field theoretical calculations [8, 9], which show that there is indeed a dynamical length scale that is predicted to diverge at T_c , the critical temperature of the mode-coupling theory [10], according to $\xi^{\text{dyn}} \propto (T - T_c)^{-0.25}$ [9, 11]. However, this prediction seems to be at odds with the results

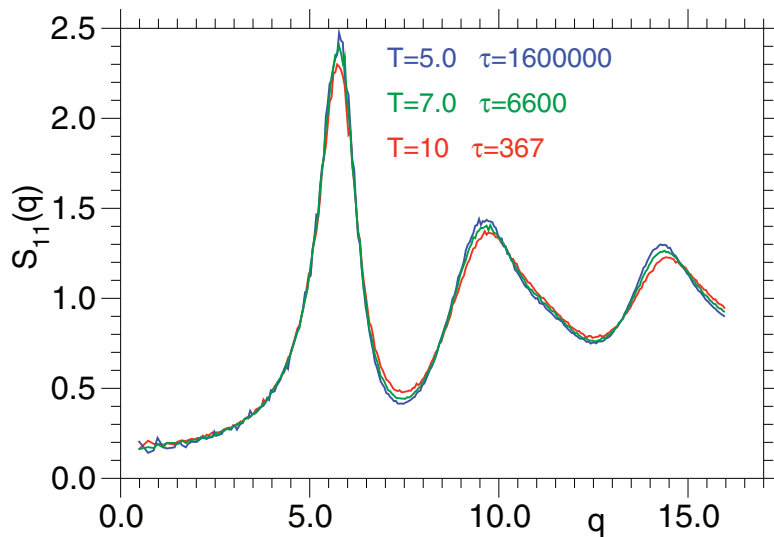


Figure 1: Partial structure factor as a function of wave-vector q for the binary system studied in this work. The three curves correspond to the temperatures given in the legend. Also given are the α -relaxation times τ of the system at the corresponding temperatures.

from experiments that do not indicate any divergence of the dynamical length scale around T_c [5, 6]. This discrepancy might be due to the fact that in experiments the dynamical length scale is determined only in a rather indirect manner, and therefore it is not evident that in real systems the dynamical length scale does indeed not show any particular signature around T_c . Another possibility could be that this prediction is not relevant outside the realm of mean field approximations and that mode-coupling calculations are of little use to interpret dynamic heterogeneities.

Another important question regarding the dynamical heterogeneities concerns the microscopic mechanism which is responsible for their existence: Are they just thermal fluctuations of the particle density or of the velocities, or do they instead reflect the emergence of some ‘special’ amorphous structures that become more extended when temperature is decreased? Experiments and simulations indicate that two-point correlation functions, such as the radial distribution function $g(r)$ or the static structure factor $S(q)$, do not show any remarkable temperature dependence, in contrast to what is found in the vicinity of second order phase transitions. As an example we show in Fig. 1 the partial structure factor of a glass-forming system (described below) at three different temperatures, demonstrating that $S(q)$ only shows a mild temperature dependence. This is in contrast with the T -dependence of the relaxation times τ (which can, e.g., be determined from the decay time of the intermediate scattering function), that change in the same T -range by a factor of about 10^4 .

Since two-point correlation functions do not show a significant T -dependence one is lead to probe higher order correlation functions. Such a line of research is also motivated by the fact that the so-called random first order transition (RFOT) theory of the glass transition predicts that glass-formers do show at low temperatures a *static* order [12, 13]. Within this theory, this order becomes relevant around the mode-coupling temperature T_c and, within mean field, is found to diverge at the ideal glass transition, also called Kauzmann temperature $T_K < T_c$.

Although computer simulations have given evidence that certain structural motifs do indeed become more frequent at low temperatures [14, 15], it is at present not clear at all whether these locally favored structures are only relevant in the moderately supercooled regime or also at temperatures close to the glass transition [16]. As a consequence there have recently been significant efforts to develop methods to define and quantify such increasing static length scales [17, 18, 19, 20, 21, 22, 23, 24, 25]. These studies are rendered difficult by the fact that the length scales are expected to become reasonably large only at temperatures around T_c , a temperature at which the dynamics of the glass-former is usually very sluggish. Hence current computer simulations have a hard time to probe the *equilibrium* dynamics of the liquid in this temperature range. Nevertheless, these efforts are highly justified since one needs to clarify how these two strong theoretical predictions, that the dynamic length scales diverges at T_c whereas the static

scale diverges only at $T_K < T_c$, compare with measurements in real systems. We want to determine if and how these two seemingly contradictory results survive in real glass-formers. In the following we will therefore present the results of large scale computer simulations in which we have addressed the question on the presence of dynamical and static length scales, how they depend on temperature, and how they are related to each other.

2. Model and Details of the Simulations

The model we are using is a 50:50 binary mixture of harmonic spheres with different sizes [26]. All particles have the same mass m and particles i and j that are a distance r_{ij} apart have an interaction given by

$$V(r_{ij}) = \frac{\epsilon}{2}(1 - (r_{ij}/\sigma_{ij})^2) \quad . \quad (1)$$

Here $\sigma_{11} = 1.0$, $\sigma_{12} = 1.2$ and $\sigma_{22} = 1.4$. In the following we will use σ_{11} as the unit of distance, $\sqrt{m\sigma_{11}/\epsilon}$ as the unit of time and $10^{-4}\epsilon$ as unit of energy, setting the Boltzmann constant $k_B = 1.0$. The equations of motion are integrated using the velocity form of the Verlet algorithm, using a time step of 0.02. We use two distinct protocols to study this system.

In a first study [22], we have equilibrated a system of 4320 particles using a box of size $L_x = L_y = 13.68$ and $L_z = 34.2$. After equilibration, we have permanently frozen the position of all the particles that had a coordinate $-1.4 \leq z \leq 0$ (using periodic boundary conditions) and introduced at $z = 0$ a hard wall. Therefore these particles become a frozen amorphous wall. It can be shown that this freezing does not influence the static properties of the remaining fluid particles [27]. We have performed a disorder average over 10-30 independent configurations of the wall. Due to the presence of an amorphous wall, this setup allows us to study how the static and dynamic properties of the liquid are influenced by the presence of the frozen particles. Since the latter occupy positions that are characteristic of the bulk liquid, this point-to-set approach probes static and dynamic bulk correlation functions. In the following we will characterize the static and dynamic properties of the system as a function of the distance z from the frozen wall.

In a second set of simulations [28], we have performed equilibrium simulations of the bulk system using various system sizes N from $N = 32$ up to $N = 16384$ keeping the density constant. For each temperature and system size we determine the bulk relaxation time, $\tau(L, T)$, and study at each temperature the effect of decreasing the system size on the bulk relaxation. Our goal is to study the interplay between a finite system size and the relevant correlation length scales characterizing the glass-former in the bulk.

3. Results

In order to characterize the static and dynamic properties of the system we introduce a coarse-grained density field in the following manner [20]. We decompose the simulation box into small non-overlapping boxes (cells) of size $\delta \approx 0.55$ and define a binary variable $n_i(t) = 1$ if at time t cell number i is occupied by at least one particle, and $n_i(t) = 0$ if not. From this coarse grained density we can now define a time correlation function, also called ‘overlap’,

$$q_c(t, z) = \left[\frac{\sum_{i(z)} \langle n_i(t)n_i(0) \rangle}{\sum_{i(z)} \langle n_i(0) \rangle} \right]_{\text{wall}} \quad , \quad (2)$$

which gives the probability that if a cell has been occupied at time $t = 0$ it is also occupied at time t . Note that in Eq. (2) the sum extends over all cells that are at distance z from the wall and $[\cdot]_{\text{wall}}$ denotes the average over the independent walls. We note that $q_c(t, z)$ is a collective quantity in the sense that we do not specify in its definition the label of the particle that occupies a given cell. It is, however, also possible to define a ‘self-overlap’, $q_s(t, z)$, by requiring that at times $t = 0$ and t a given cell is occupied by the same particle and below we will discuss this correlator as well.

In Fig. 2 we show the time dependence of $q_c(t, z)$ for different values of z . The three panels correspond to different temperatures. We see that at high temperatures (Fig. 2a) $q_c(t, z)$ decays quite quickly to a z -dependent constant. This decay is very fast for intermediate and large values of z , whereas it is slower for small values of z . Thus we see that at this temperature the density correlation function relaxes quickly and becomes independent of z for large distances from the frozen wall and that the relaxation dynamics slows down if the wall is approached, in agreement with previous

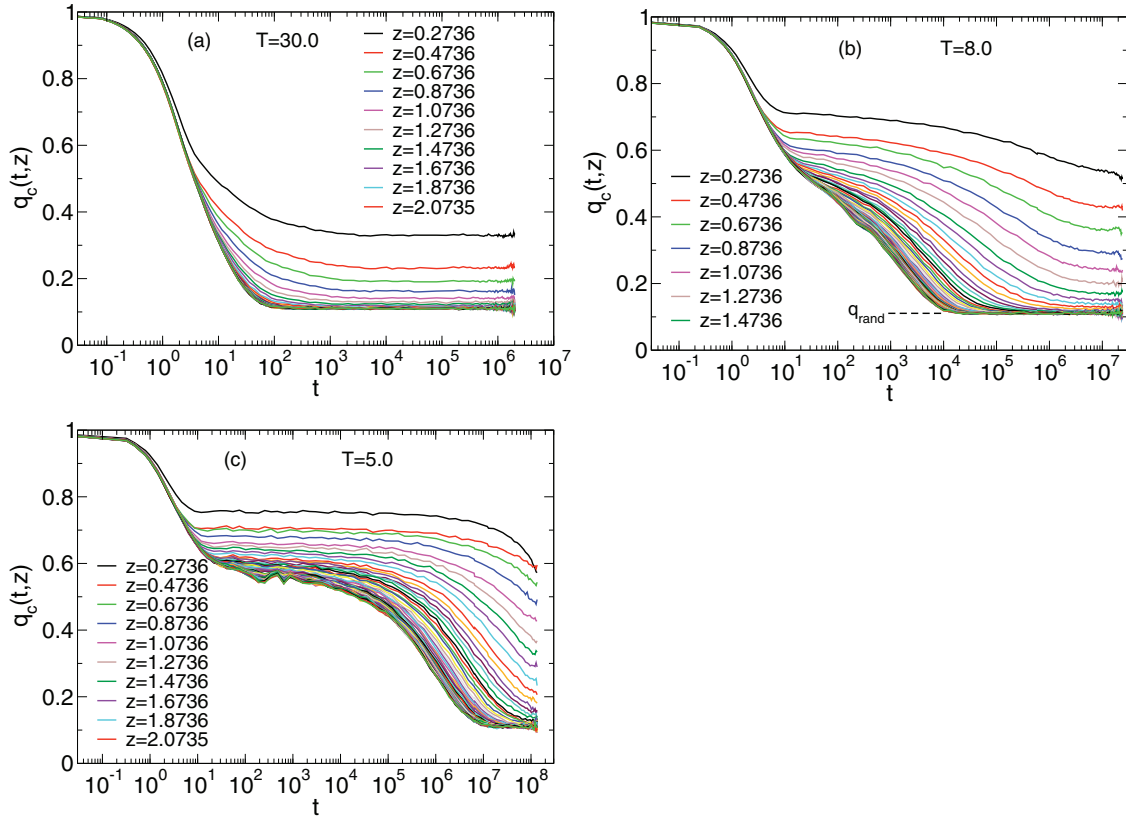


Figure 2: Time dependence of the correlation function $q_c(t, z)$ as defined in Eq. (2) for different values of z . The three panels correspond to the temperatures given in the figures.

findings [27]. If T is decreased to a temperature at which the relaxation dynamics of the bulk system starts to become somewhat sluggish [26] one finds qualitatively the same results (Fig. 2b). The main difference is that for this T the correlation function shows for all values of z at intermediate times a plateau, a feature that is well known from the relaxation dynamics in the bulk and that corresponds to the temporary trapping of the particles inside the cage formed by their neighbors [7]. From the figure we recognize that the width of this plateau increases with decreasing z , i.e. the trapping becomes more pronounced if one approaches the wall. This effect is related to the fact that the particles constituting the walls do not have any thermal motion and hence do not provide any fluctuations that can help the particles inside the liquid to relax. This effect becomes even stronger if temperature is lowered further, Fig. 2c. At this temperature, which is somewhat below the critical temperature of mode-coupling theory [22], the relaxation dynamics close to the wall is so slow that it is not possible to see the final relaxation within the time window of our simulation. This does not imply that our simulations are out of equilibrium since, by construction of the wall, we have started our production runs with an equilibrated state. It implies, however, that we cannot accurately extract the long-time limit of these overlap functions for all values of z .

From Fig. 2 we see that at intermediate and long times $q_c(t, z)$ can be approximated by the functional form

$$q_c(t, z) = A(z, T) \exp[-(t/\tau_c(z, T))^{\beta(z, T)}] + q_\infty(z, T) + q_{\text{rand}}. \quad (3)$$

Here q_{rand} is the long time value of $q_c(t, z)$ for large z , i.e. it is a quantity that can be obtained with high precision from a simulation of the bulk. We find that $q_{\text{rand}} \approx 0.110595$, independently of T . Therefore, the quantity $q_\infty(z, T)$ quantifies the nontrivial influence of the wall on the local density field. Qualitatively this influence can be seen in Fig. 3 where we show the superposition of many particle configurations obtained during a run that extended over about 100 times the typical relaxation time of the bulk system. In order to avoid overcrowding we show only a thin slice of the system, i.e. the particles that have coordinates $0 \leq x \leq 1.0$. From these figures we see that far from the wall the system is fully ergodic, and particles fill out all the available space in a uniform manner. By contrast,

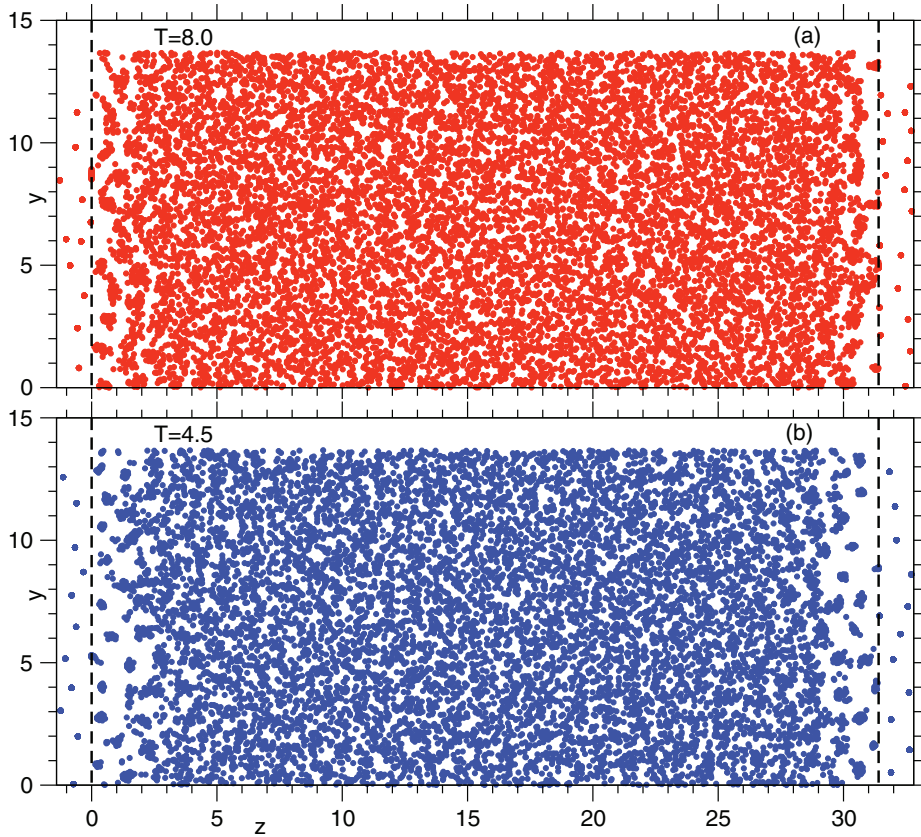


Figure 3: Superposition of snapshots of the system at $T = 8.0$ and $T = 4.5$ (panel (a) and (b), respectively). The vertical dashed lines show the location of the hard walls. Only particles in the slab $0 \leq x \leq 1.0$ are shown. Individual snapshots are separated by about $\tau_{\text{bulk}}(T)$ and the total time is about $100\tau_{\text{bulk}}(T)$.

the space close to the wall is occupied in a very heterogeneous manner, exhibiting locations in which there is a high probability to find a particle and others in which this probability is small. A comparison of the two panels shows that the length scale over which the wall influences the local structure increases if temperature is decreased, thus giving rise to an increasing static length scale.

We find that the self-overlap $q_s(z, t)$ shows a qualitatively similar time dependence as $q_c(z, t)$. The main difference is that at long times the former always decays to zero since the probability that a given cell is occupied at very long times by the particle that was present at time zero becomes negligibly small. Therefore the quantity $q_\infty(z, T)$, now associated to $q_s(z, t)$, is zero for all values of z and T .

The increasing influence of the wall on the local structure of the liquid can be quantified by the static overlap $q_\infty(z, T)$ from Eq. (3), which gives the excess probability to find a particle in a given cell with respect to the bulk probability. This quantity can be obtained with quite high precision by fitting the final decay of $q_c(t, z)$ with the functional form given in Eq. (3) and in Ref. [22] we have shown that this expression does indeed give a very good description to the data. The resulting z -dependence of $q_\infty(z, T)$ is shown in Fig. 4. We see that for all temperatures investigated $q_\infty(z, T)$ is compatible with an exponential dependence in z (straight lines):

$$q_\infty(T) = B(T) \exp(-z/\xi^{\text{stat}}(T)). \quad (4)$$

This functional form allows us thus to define a T -dependent “point-to-set” length scale ξ^{stat} that grows if the temperature is decreased. Note that the data points imply that not only ξ^{stat} depends on T but the prefactor B from Eq. (4) does as well since the curves move upwards with decreasing T . This suggests to define a second static length scale $\xi^{\text{stat-int}}$ via the integral of $q_\infty(T)$ which, with Eq. (4), leads to the estimate

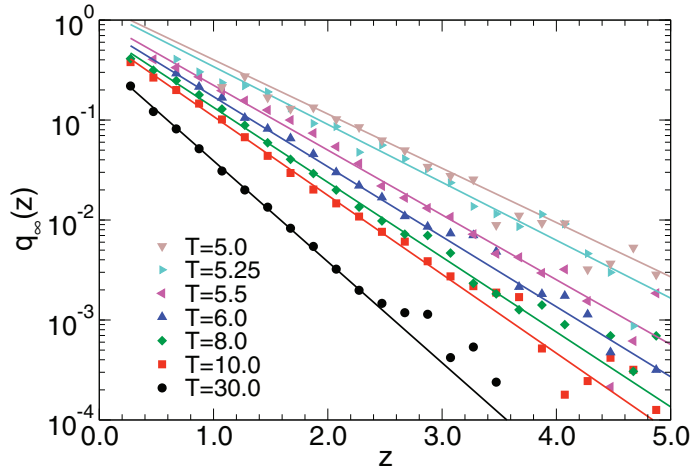


Figure 4: z -dependence of the long-time overlap for different temperatures (symbols). The straight lines are fits with an exponential.

$$\xi^{\text{stat-int}} \approx B(T) \cdot \xi^{\text{stat}}. \quad (5)$$

Before discussing the temperature dependence of these static length scales we briefly turn our attention to the dynamics. From the fit to the data with the functional form given by Eq. (3) we can extract a relaxation time $\tau_c(z, T)$ as well as its single particle counterpart, $\tau_s(z, t)$, corresponding to the self overlap. In Fig. 5a we show the z -dependence of $\tau_s(z, t)$, i.e. the relaxation times extracted from the self-overlaps. (The data from the collective functions look qualitatively similar). We see that for all temperatures the relaxation times become independent of z if z is large which shows that the size of the simulation box is sufficiently large to reach the bulk value. For small distances from the wall the relaxation times quickly increase and the z -range over which this increase can be noticed increases with decreasing temperature. This observation implies that there is a *dynamic* length scale that growth if T is lowered. Previous studies for a Lennard-Jones system have shown [27] that the z -dependence of $\tau_s(z, T)$ can be approximated well by

$$\log(\tau_s) = \log(\tau_s^{\text{bulk}}) + B_s(T) \exp(-z/\xi_s^{\text{dyn}}). \quad (6)$$

That this functional form does give a good description of the data also for the present system is shown in Fig. 5b. We

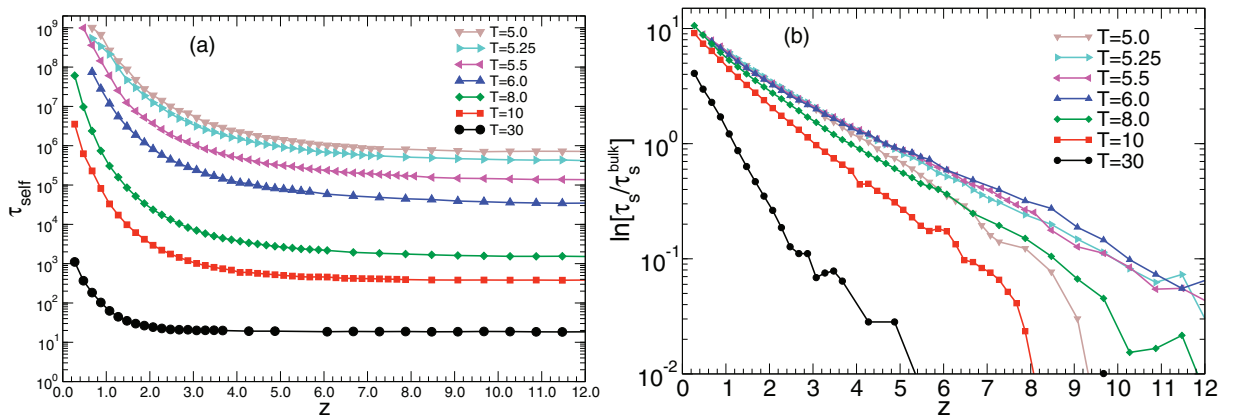


Figure 5: a) z -dependence of the relaxation time as obtained for the self-overlap. The different curves correspond to different temperatures. b) Same data as in panel a) but plotted in a form to show that at intermediate and large z the data is compatible with the functional form given by Eq. (6).

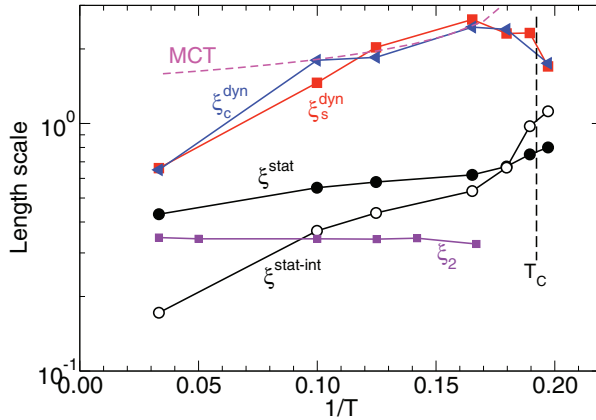


Figure 6: Temperature dependence of different static and dynamic length scales. The vertical dashed line indicates $T_c = 5.2$.

see that for intermediate and large values of z the data points are indeed compatible with a straight line, as expected from Eq. (6). Therefore we can use this result to define a dynamic length scale ξ_s^{dyn} .

A close inspection of the data shows that the slope of the curves at intermediate and large z does *not* evolve monotonically with temperature. Instead the data for $T = 6.0$ has the smallest slope and the ones for $T = 5.25$ and $T = 5.0$ have a larger slope (in absolute values). This observation implies that the dynamic length scale is not a monotonically increasing function of T but instead shows a maximum. In Ref. [22] we have shown that this surprising result is not just an artifact of our data analysis because it can be seen directly in the time correlation functions and therefore must be considered as a real effect. Finally we also note that for small values of z the curves $\tau_s(z, T)/\tau_s(\text{bulk}, T)$ become independent of T . This implies that very close to the wall the temperature dependence of the relaxation dynamics tracks the one of the bulk system. These two results give indirect evidence that the relaxation dynamics occurs on *two* different length scales: A first one that is relevant at short scales and a second one, ξ_s^{dyn} , that operates at intermediate and long distances. We will come back to this interpretation below.

In Fig. 6 we summarize the T -dependence of the various static and dynamic length scales. The length scale labeled $\xi_2(T)$ has been obtained by fitting the decay of the envelope of the radial distribution function $g(r)$ for the larger particles to an exponential. As expected, this length scale shows basically no T -dependence, in agreement with the data shown in Fig. 1. As discussed in the context of Fig. 4, our simulations allow to extract two static length scales that are related to multi-point correlations: ξ^{stat} and $\xi^{\text{stat-int}}$. The influence of the particles constituting the wall is likely to be associated with $\xi^{\text{stat-int}}$, but one can expect that at very low temperatures (at present inaccessible to computer simulations) the two scales coincide because the prefactor $B(T)$ should saturate. From Fig. 6 we see that both scales increase with decreasing temperature and that $\xi^{\text{stat-int}}$ does show a stronger T -dependence than ξ^{stat} . This latter behavior is related to the fact that the prefactor B in Eq. (4) also shows a significant T -dependence. From the figure we see that the so defined static length scales are at intermediate and low temperatures significantly larger than the one obtained from the two point correlation function, thus showing that multi-point correlations are indeed of high interest for glass-forming systems.

Also included in the figure are the dynamic length scales ξ_s^{dyn} as determined from the collective and self overlaps. We see that within the numerical noise of the data these two scales coincide and that both of them are significantly larger than the static ones. (Qualitatively similar results have been obtained for different geometries of pinned particles, which indicates that this result is quite general [23].) The growth of the dynamic length scales for $T > T_c$ (where the critical temperature T_c from the mode-coupling theory is indicated by a vertical dashed line) is compatible with the prediction from mode-coupling theory [11], i.e. the functional form $\xi_s^{\text{dyn}} \sim (T - T_c)^{-0.25}$ with $T_c = 5.2$ (dashed line). (See Ref. [22] on how T_c has been determined.) But in view of the uncertainty in the value of T_c and the smallness of the exponent, this is not a very strong statement. More important is the observation that these dynamic length scales show a local maximum and that the temperature at which it occurs is close to the critical temperature of mode-coupling theory. This result is thus a strong evidence that around T_c the nature of the process that is responsible for the relaxation dynamics changes. Note that, in contrast to all previous investigations on the relaxation dynamics

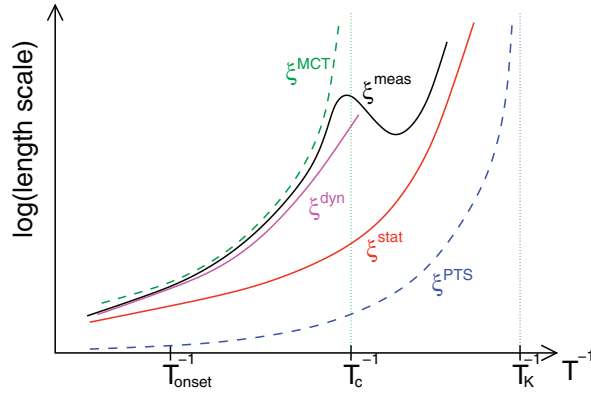


Figure 7: Schematic plot of the temperature dependence of different static and dynamic length scales.

of glass-forming liquids, the presence of the maximum is determined without using any of the mode-coupling theory predictions. It represents therefore a genuine physical phenomenon and not, for instance, deviation from a fitting formula. We interpret this maximum as a firm evidence that T_c is indeed a physically meaningful crossover temperature for the glass-former and not merely a fitting parameter.

Although the present simulations do not really permit to draw conclusions on the nature of the relaxation process at play in the various temperature regimes, we can speculate about this issue. The most natural interpretation of these data is that dynamic heterogeneity, and therefore structural relaxation, change nature when T is decreased across the mode-coupling crossover. Based on the mean field picture, we suggest the following scenario. At high temperatures (i.e. in the normal liquid state well above T_c) the particles relax in an independent manner and the dynamic and static length scales are small. If T is lowered to a temperature at which the system starts to become sluggish (i.e. below a temperature that is often called ‘onset temperature’, T_{onset}) particle motion becomes more collective and spatially correlated, as predicted for instance by mode-coupling calculations. When temperature is lowered towards T_c , however, two mechanisms start to compete. At low temperature, dynamics becomes slower and spatially correlated over a dynamic correlation length that keeps increasing, ξ^{dyn} . At the same time, close to T_c static correlations also start to become relevant and might control the dynamic profiles we observe very close to the wall. Finally, when decreasing temperature below T_c , the mode-coupling relaxation processes start to disappear (T_c is just a crossover), but static correlations remain and are now fully responsible for the dynamic profiles. In Fig. 7, we represent schematically the consequence of this scenario for length scales. We show both diverging length scales predicted within (mean field) RFOT, the dynamic length scale of mode-coupling theory ξ^{MCT} at T_c , and the static point-to-set length scale ξ^{PTS} at T_K . In finite dimensions, ξ^{dyn} is controlled by ξ^{MCT} over the regime $T_{\text{onset}} > T > T_c$, but this process progressively disappears near T_c . Static correlations ξ^{stat} , are controlled by the point-to-set correlation functions. As a result, the measured dynamic lengthscale, ξ^{meas} , is first controlled by ξ^{dyn} and then by ξ^{stat} at lower temperature, and thus ξ^{meas} exhibits a non-monotonic temperature dependence. This scenario naturally explains the emergence of a non-monotonic temperature evolution of the measured dynamic profile. We note that Stevenson *et al.* in Ref. [29] have suggested a similar scenario and have additionally proposed that the geometry of spatial correlations changes from a fractal, string-like structure above T_c , to more compact domains at lower temperatures. Our data are not incompatible with these ideas, but they do not provide direct geometric information about dynamic correlations.

The above results have been obtained for a very specific point-to-set geometry using flat amorphous walls and one may wonder about their relevance for bulk dynamics. We now briefly discuss how the non-monotonic T -dependence of ξ^{meas} can be used to understand some finite size effects of the relaxation dynamics. In Fig. 8 we show the system size dependence of the relaxation time for different temperatures, $\tau(L, T)$ for the same harmonic sphere system as the one studied near the wall. The relaxation time is defined as the time it takes for the intermediate scattering function to decay to $1/e$ of its $t = 0$ value.

The data show that at high temperatures there is no dependence on system size L , which is reasonable since all the relevant length scales are small. With decreasing T , i.e. $T = 10.0, 8.0$, and 6.0 , one finds that τ increases if L decreases, indicating that there are relaxation processes that extend over scales that become larger and compete with the finite

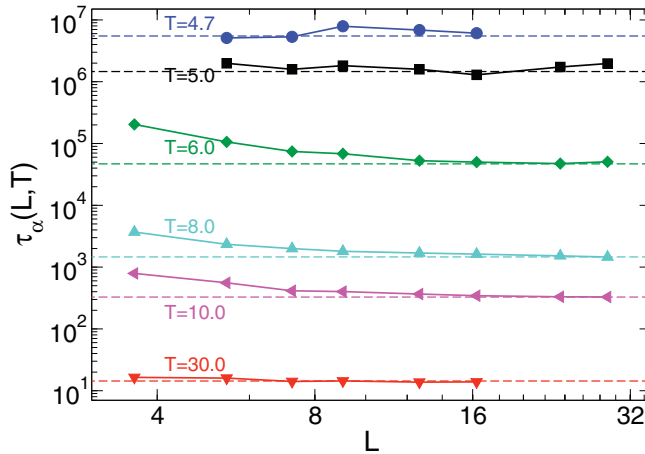


Figure 8: Relaxation time as a function of the box size for different temperatures.

system size. The temperature evolution of these data are compatible with the existence of a growing dynamic length scale in this regime. Interestingly, this effect is most pronounced for $T = 6.0$, i.e. at the temperature at which we find in Fig. 6 the maximum in ξ^{dyn} . Remarkably, by decreasing further the temperature in the regime where ξ^{dyn} was found to decrease, we find that the system size dependence of the relaxation time becomes less pronounced. Finally, at even lower temperature, $T = 4.7$, the L dependence of the relaxation time qualitatively changes nature, in agreement with the idea that dynamic process above and below T_c are qualitatively different. Thus, the non-monotonic temperature evolution of ξ^{meas} near the amorphous wall is mirrored by a similarly non-monotonic temperature evolution of the size dependence of the relaxation time in the bulk, which we see as an independent confirmation of the speculative scenario described by Fig. 7.

4. Summary

The above results show that the point-to-set protocol of freezing a finite set of particles in their equilibrium allows one to gain information about relevant static and dynamic correlation functions in glass-forming liquids. This approach opens the door to probe high order static and dynamic length scales in a novel manner. We have found that there is indeed a dynamic length scale that increases in qualitative agreement with the mean field scenario, but that this scale decreases again if one is significantly below the mode-coupling temperature. This result, which has allowed to see a signature of T_c without using any of the standard fitting procedures, gives thus support to the theoretical calculations, and suggests how the mean field predictions should be modified in finite dimensions. We hope that experiments will take up this approach and therefore confirm the scenario we have developed here.

Acknowledgments: We thank G. Biroli and A. Cavagna for fruitful exchanges about this work, and the Région Languedoc-Roussillon (L.B.), ANR DYNHET (L.B. and W.K.), and MICINN (Project: MAT2009-13155-C04-02) and Junta de Andalucía (Project: P07-FQM-02496) (S.R.V.) for financial support. W.K. is member of the Institut universitaire de France.

- [1] W. Kob, C. Donati, S. J. Plimpton, S. C. Glotzer, and P. H. Poole, *Phys. Rev. Lett.* **79**, 2827 (1997).
- [2] M. D. Ediger, *Annu. Rev. Phys. Chem.* **51** 99 (2000).
- [3] L. Berthier, *Phys. Rev. E* **69**, 020201 (2004).
- [4] *Dynamical heterogeneities in glasses, colloids, and granular media*, Eds.: L. Berthier, G. Biroli, J.-P. Bouchaud, L. Cipelletti, and W. van Saarloos, (Oxford University Press, Oxford, 2011).
- [5] L. Berthier, G. Biroli, J.-P. Bouchaud, L. Cipelletti, D. El Masri, D. L'Hôte, F. Ladieu, and M. Pierno, *Science* **310**, 1797 (2005).

- [6] C. Dalle-Ferrier, C. Thibierge, C. Alba-Simionesco, L. Berthier, G. Biroli, J.-P. Bouchaud, F. Ladieu, D. L'Hôte, and G. Tarjus, *Phys. Rev. E* **76**, 041510 (2007).
- [7] K. Binder and W. Kob, *Glassy materials and disordered solids, 2nd edition* (World Scientific, Singapore, 2011).
- [8] G. Biroli and J. P. Bouchaud, *Europhys. Lett.* **67**, 21 (2004).
- [9] S. Franz and A. Montanari, *J. Phys. A: Math. Theor.* **40**, F251 (2007).
- [10] W. Götze, *Complex dynamics of glass-forming liquids: A mode-coupling theory* (Oxford University Press, Oxford, 2008).
- [11] G. Biroli, J.-P. Bouchaud, K. Miyazaki, and D. R. Reichman, *Phys. Rev. Lett.* **97**, 195701 (2006).
- [12] T. R. Kirkpatrick, D. Thirumalai, and P. G. Wolynes, *Phys. Rev. A* **40**, 1045 (1989).
- [13] X. Y. Xia and P. G. Wolynes, *Proc. Natl. Acad. Sci. USA* **97**, 2990 (2000).
- [14] D. Coslovich and G. Pastore, *J. Chem. Phys.* **127**, 124504 (2007).
- [15] H. Tanaka, T. Kawasaki, H. Shintani, and K. Watanabe, *Nature Mat.* **9**, 324 (2010).
- [16] G. Tarjus, S. A. Kivelson, Z. Nussinov, and P. Viot, *J. Phys. Condens. Matter* **17**, R1143 (2005).
- [17] J.-P. Bouchaud and G. Biroli, *J. Chem. Phys.* **121**, 7347 (2004).
- [18] R. L. Jack and J. P. Garrahan, *J. Chem. Phys.* **123**, 164508 (2005).
- [19] A. Cavagna, T. S. Grigera, and P. Verrocchio, *Phys. Rev. Lett.* **98**, 187801 (2007).
- [20] G. Biroli, J.-P. Bouchaud, A. Cavagna, T. S. Grigera, and P. Verrocchio, *Nature Phys.* **4**, 771 (2008).
- [21] M. Mosayebi, E. Del Gado, P. Ilg, and H. C. Öttinger, *Phys. Rev. Lett.* **104**, 205704 (2010).
- [22] W. Kob, S. Roldan-Vargas, and L. Berthier, *Nature Phys.* **8**, 164 (2012).
- [23] L. Berthier and W. Kob, *Phys. Rev. E* **85**, 011102 (2012).
- [24] R. L. Jack and L. Berthier, *Phys. Rev. E* **85**, 021120 (2012).
- [25] B. Charbonneau, P. Charbonneau, and G. Tarjus, *Phys. Rev. Lett.* **108**, 035701 (2012).
- [26] L. Berthier and T. A. Witten, *EPL* **86**, 10001 (2009); *Phys. Rev. E* **80**, 021502 (2009).
- [27] P. Scheidler, W. Kob, and K. Binder, *Europhys. Lett.* **59**, 701 (2002); *J. Phys. Chem. B* **108**, 6673 (2004).
- [28] L. Berthier, G. Biroli, D. Coslovich, W. Kob and C. Toninelli, in preparation.
- [29] J. D. Stevenson, J. Schmalian, and P.G. Wolynes *Nature Phys.* **2**, 268 (2006).